

Ensemble empirical mode decomposition for analyzing phenological responses to warming



Biing T. Guan*

School of Forestry and Resource Conservation, National Taiwan University, 1, Section 4, Roosevelt Road, Taipei 10617, Taiwan, ROC

ARTICLE INFO

Article history:

Received 28 October 2013

Received in revised form 12 March 2014

Accepted 14 March 2014

Keywords:

Climate warming

Ensemble empirical mode decomposition

Phenophase shifts

Phenophase variability

ABSTRACT

Numerous studies conducted over the past decade have revealed that plant phenophases have shifted in many temperate ecosystems. Although the consensus is that these shifts reflect plant responses to rise in temperatures, we have yet to match unequivocally the phenological and temperature trends. More importantly, little is known about warming's effects on and contributions to phenophase variability. The key to accomplishing both tasks lies in a proper separation of a trend from natural variability. Based on ensemble empirical mode decomposition, this study shows that, over the past 30 years, the advancing trends in the first flowering dates (FFD) of apple (*Malus domestica*) in Austria and blackthorn (*Prunus spinosa*) in Germany unequivocally correspond to the respective regional winter/spring warming trends. The variability of both FFD series before 1981 was almost entirely due to natural variability. In contrast, warming since 1981 contributed 4% and 21% toward the total phenophase variability of apple and blackthorn, respectively. Furthermore, while contributing to both the temperature and FFD overall variability, recent warming also lowers the FFD natural variability by modulating the temperature natural oscillation amplitudes. Thus, warming can affect both the timing and the natural variability of a phenophase development. As concurrently shifting the timings and reducing the natural variability of phenophase developments may have important ecological and evolutionary consequences, it will be of great interest and importance to examine whether the conclusion holds for other phenophases and species in various regions as well. The introduced approach will be a valuable tool for answering the question.

© 2014 Elsevier B.V. All rights reserved.

1. Introduction

Analyses based on spatially extensive phenological data have revealed that in many temperate ecosystems, plant phenophases have shifted (Parmesan and Yohe, 2003; Root et al., 2003), especially those of spring events (Badeck et al., 2004; Schwartz et al., 2006). These shifts could potentially generate a chain of adverse effects that would cascade throughout ecosystems (Memmott et al., 2007; Walther, 2010; Donnelly et al., 2011; Diez et al., 2012). Because plant phenophase variations mainly reflect thermal environment variability in temperate ecosystems, the consensus is that such shifts are biological responses to anthropogenic

warming (Cleland et al., 2007; Rosenzweig et al., 2008; Parmesan et al., 2011).

Temperature variability may arise from both natural variability and human activity (Badeck et al., 2004; Rosenzweig et al., 2008; Polgar and Primack, 2011). By definition, the influences of the former on temperature (and thus, plant phenophase developments) should be oscillatory, whereas those of the latter should be a non-cyclic trend over the time span considered. Otherwise, we cannot distinguish these types of influences from one another. In practice, however, low-frequency natural variation could complicate the matter, as a portion of the variation might resemble and therefore be indistinguishable from a trend caused by anthropogenic forcing. Notwithstanding the cause of recent warming, be it anthropogenic or natural variability, if this warming is indeed responsible for the observed plant phenophase shifts, then the trends of phenophase development and recent warming should correspond closely.

However, although significant progress has been achieved in identifying and quantifying phenophase shifts (e.g., Dose and Menzel, 2006; Menzel, 2006; Parmesan, 2007; Schleip et al., 2008; Amano et al., 2010), an unequivocal correspondence between these two types of trends remains to be demonstrated. More importantly,

Abbreviations: edf, effective degrees of freedom; EEMD, ensemble empirical mode decomposition; EMD, empirical mode decomposition; FFD, first flowering dates; IMF, intrinsic mode function; NAO, Northern Atlantic Oscillation; OC, oscillatory component; SSA, singular spectrum analysis; T_{\max} , monthly mean of the daily maximum temperature; T_{mean} , monthly mean of the daily mean temperature.

* Tel.: +886 2 3366 4628; fax: +886 2 2363 9247.

E-mail address: btguan@ntu.edu.tw

Table 1
Summary of phenological and temperature data.

Series	Phenological records				
	Site	Longitude (°E)	Latitude (°N)	Elevation (m)	Period
Apple	Weiz, Austria	15.63	47.22	465	1951–2003
Blackthorn	Germany ^a	8.65–10.47	49.42–50.95	190–290	1951–2011
	Average February to April T_{\max} ^b				
T_{\max} -A	Austria	13.0–16.0	47.0–49.0		1951–2011
T_{\max} -G	Germany	8.5–10.5	49.0–51.0		1951–2011

^a A composite series from eight stations. See Appendix A for the details.

^b Based on the European Climate Assessment & Dataset Ensembles Observations E-OBS 5.0 gridded dataset, resolution 0.25°.

we have yet to examine warming's effects on and contributions to phenophase variability. Because changes in phenophase variability can have important ecological and evolutionary consequences (Diez et al., 2012), such an undertaking is crucial for our understanding and assessment of how warming affects ecosystems.

The key to accomplishing both tasks lies in a proper separation of a trend from natural variability (i.e., oscillatory component, OC). Three interrelated issues, however, have impeded us from achieving the goal until recently. First, both phenophase development and temperature exhibit substantial year-to-year variability (Badeck et al., 2004; Polgar and Primack, 2011), which makes it difficult to identify and extract the embedded trends. Second, phenological and temperature data are typically non-linear and non-stationary, which renders the classical time series methods invalid. Third, it is preferable and more acceptable if no external information (e.g., an *a priori* model structure) is injected during the separation process.

A potentially useful approach for separating a trend from OC embedded in temperature and phenological data is ensemble empirical mode decomposition (EEMD; Wu and Huang, 2009). EEMD is an improvement of empirical mode decomposition (EMD), an empirical but highly efficient and adaptive method for processing non-linear and non-stationary signals (Huang et al., 1998; Huang and Wu, 2008). As a part of the Hilbert–Huang transform, EMD views a complex signal as superimpositions of a finite and small number of simple intrinsic oscillatory functions (the intrinsic mode functions, IMFs) with significantly different frequencies and a residual (trend). EMD seeks to separate the IMFs and trend adaptively and intrinsically in time domain, while satisfying the completeness, orthogonality, and uniqueness properties required by a decomposition method (Huang and Wu, 2008).

Using two long-term European first flowering date (FFD, day of the year) series and the corresponding regional winter/spring temperature data as examples, this study shows that EEMD can resolve the three issues simultaneously and demonstrates how the phenophase timings and variability responded to recent warming.

2. Materials and methods

2.1. Phenological data

The apple (*Malus domestica*, medium cultivar) FFD anomaly series (1951–2003) was obtained in Weiz, Austria (Pan European Phenology station ID 6594; Table 1 and Fig. 1) and with respect to the 1961–1990 base period mean FFD (the 117th day of the year). The FFD of this species is considered to be controlled by spring temperature alone (Cook et al., 2012).

The blackthorn (*Prunus spinosa* L.) FFD anomaly series (1951–2011) was the annual average of 8 German FFD series (Table 1, Fig. 1, and Appendix A), without adjusting for elevation differences and with respect to the 1961–1990 base period mean FFD (the 110th day of the year). In contrast to apple, the FFD of blackthorn is considered to be controlled by both spring and previous fall/winter temperatures (Cook et al., 2012).

The FDD data were from the PEP725 Pan European Phenology Project (2012) data archive. For the species and regions examined, this study only included stations with uninterrupted observations in analyses.

2.2. Climate data

The February to April (FMA) thermal regime plays a large role in governing the spring phenophase development of plants in Europe (Chmielewski and Rötzer, 2001; Menzel, 2003; Dose and Menzel, 2006; Amano et al., 2010). It has been suggested in the literature that the spring phenophase development of plants in Europe is controlled by the average FMA monthly mean of the daily mean temperature (T_{mean}). A preliminary analysis, however, indicated that the FFD of both species had a stronger correlation with the average FMA monthly mean of the daily maximum temperature (T_{max}) than with T_{mean} . Thus, this study examined two long-term (1951–2011), regional average FMA T_{max} anomaly series (base period 1961–1990), denoted T_{max} -A and T_{max} -G for the apple and blackthorn study regions, respectively (Table 1 and Fig. 1).

The Northern Atlantic Oscillation (NAO) is a major natural climate phenomenon that influences the winter/spring temperature and plant spring phenophase developments in Europe (Jones et al., 1997; Chmielewski and Rötzer, 2001; Menzel, 2003; Osborn, 2011). Hence, this study examined the correlations between the NAO Gibraltar–Stykkishólmur (NAO_{GS}) index and the four anomaly series as well.

The average FMA T_{max} anomaly series were derived from the E-OBS 5.0 gridded T_{max} datasets (0.25° resolution) from the EU-FP6 ENSEMBLES project (Haylock et al., 2008). All of the gridded datasets and the NAO_{GS} index were obtained from the Royal Netherlands Meteorological Institute Climate Explorer website (<http://climexp.knmi.nl>).

2.3. Ensemble empirical mode decomposition

Let $x(t)$ be a time series, and the objective of EMD is to decompose $x(t)$ into a small and finite number of IMFs and a residual (trend), that is, $x(t) = \sum_{i=1}^k \text{IMF}_i(t) + R(t)$, where k is the number of IMFs, $\text{IMF}_i(t)$ is the i th IMF, and $R(t)$ is the residual or trend. The number of IMFs is a function of data length, $k = \log_2(\text{length}) - 1$, rounded toward zero. An IMF is an oscillatory function that satisfies the conditions (1) the numbers of extrema and zero crossings must be equal or differ at most by one, and (2) the envelopes defined by the local maxima and minima average to zero (Huang et al., 1998; Huang and Wu, 2008).

The IMFs are extracted from high to low frequencies using a spline-based iterative sifting process. EMD first finds the local extrema in $x(t)$ and generates a pair of upper and lower envelopes by interpolating local maxima and local minima using a cubic spline. It then takes the average of the two envelopes and subtracts the average from the original signal $x(t)$, producing an oscillatory series $x'(t)$. Treating $x'(t)$ as the new signal and by repeating the

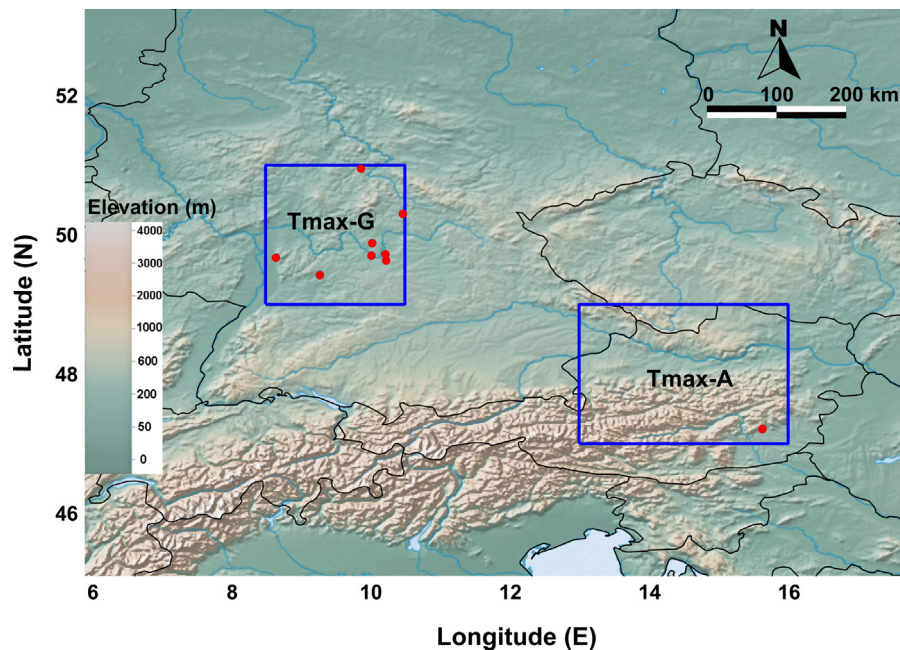


Fig. 1. Map of the study regions. Dots indicate the locations of the PEP725 Pan European Phenology Project stations providing records used in the study. The boxes denote the regions from which the average FMA T_{\max} data included in the analyses were obtained based on the EOB-S 5.0 gridded temperature field. (Map is made with Natural Earth).

local envelopes finding-averaging-subtracting (sifting) steps, $x'(t)$ is further processed until it meets the requirements of an IMF.

Once an IMF is extracted, EMD subtracts it from $x(t)$ and sifts through the remaining part of the signal to extract the next IMF of lower frequency. The sifting process runs iteratively until the remaining signal is either constant, monotonic, or contains only one extremum over the data span considered, the $R(t)$ part of the decomposition (Huang et al., 1998; Huang and Wu, 2008).

Developed to alleviate the signal intermittence problem in EMD, EEMD is a Monte Carlo approach in which zero-mean Gaussian white noise is added to each EMD process to achieve better signal separation. An EEMD IMF or trend is the ensemble mean of the corresponding EMD IMFs or trends (Wu and Huang, 2009).

Because EMD/EEMD decomposes time series based on local behaviors and in a sequential manner, there is no need to assume either the linearity or stationarity in data. It also does not require an *a priori* structure about the trend, the trend is derived intrinsically and adaptively (Wu et al., 2007). These properties make EEMD an ideal tool for OC-trend separations.

EEMD is not the only approach in time series decomposition that can accomplish a proper OC-trend separation without assuming stationarity, linearity, or a model structure. For example, singular spectrum analysis (SSA) commonly used in climate science research (Hudson and Keatley, 2010; Golyandina and Zhigljavsky, 2013), or smoothing spline based on a roughness penalty, of which the Hodrick–Prescott filter commonly used in econometrics is a special case (Paige and Trindade, 2010), can also be employed for the task. Hudson and Keatley (2010) applied SSA to analyze the flowering phenology of four eucalypt species.

However, EMD/EEMD does offer certain advantages. For example, SSA requires users to specify a window length parameter, which can significantly affect the outcomes. After initial decomposition, SSA also requires reconstruction step to achieve separation (Hudson and Keatley, 2010; Golyandina and Zhigljavsky, 2013). Smoothing spline will not work well if residuals are serially correlated. Moreover, smoothing spline cannot separate the OC of a time series into subcomponents representing oscillations of different frequencies. This capability is included by design in both EEMD

and SSA. Although this capability is not directly relevant to this study, it is necessary for assessing how natural climate phenomena of different frequencies (e.g., El Niño–Southern Oscillation or NAO) affect temperature regimes and phenophase developments.

The decomposition was based on the EEMD MATLAB codes provided by the Research Center for Adaptive Data Analysis of the National Central University of Taiwan (available at http://rcada.ncu.edu.tw/research1_clip_program.htm). Each EEMD run comprised 5000 EMD runs. The standard deviation of the introduced Gaussian white noise was 0.05 of that of the FFD series and 0.8 of that of the average FMA T_{\max} series. For each EEMD decomposition, each anomaly series was decomposed into an OC (*i.e.*, the sum of the EEMD IMFs) and a trend. This study required that the resulting trend met the definition.

2.4. Statistical analyses

Variances of the anomaly series and the EEMD-extracted OCs were calculated for the entire data span as well as for the split periods before and after 1981 (hereafter denoted as P1 and P2, respectively). To determine the relative contribution of an extracted trend toward the observed variability of a series, a principal component analysis (PCA) was applied to the two EEMD-extracted components of each anomaly series over the entire data span and over the split periods separately.

Simple linear regressions were used to estimate the temperature sensitivities of FFD OCs with respect to the corresponding average FMA T_{\max} OCs. Tests of slope homogeneity based on a general linear model approach were used to examine whether the temperature sensitivities and the responses of the OCs to the NAO were the same in the split periods.

In correlating two trends, one way to account for serial correlation is to adjust for the loss of degrees of freedom. This study estimated the effective degrees of freedom (edf) of the correlation based on the formula $n' = n(1 - r_1 r_2) / (1 + r_1 r_2)$, where n' is the estimated edf, n is the number of observations, and r_1 and r_2 are the 1st-order autocorrelation coefficients of the two trends (Dawdy

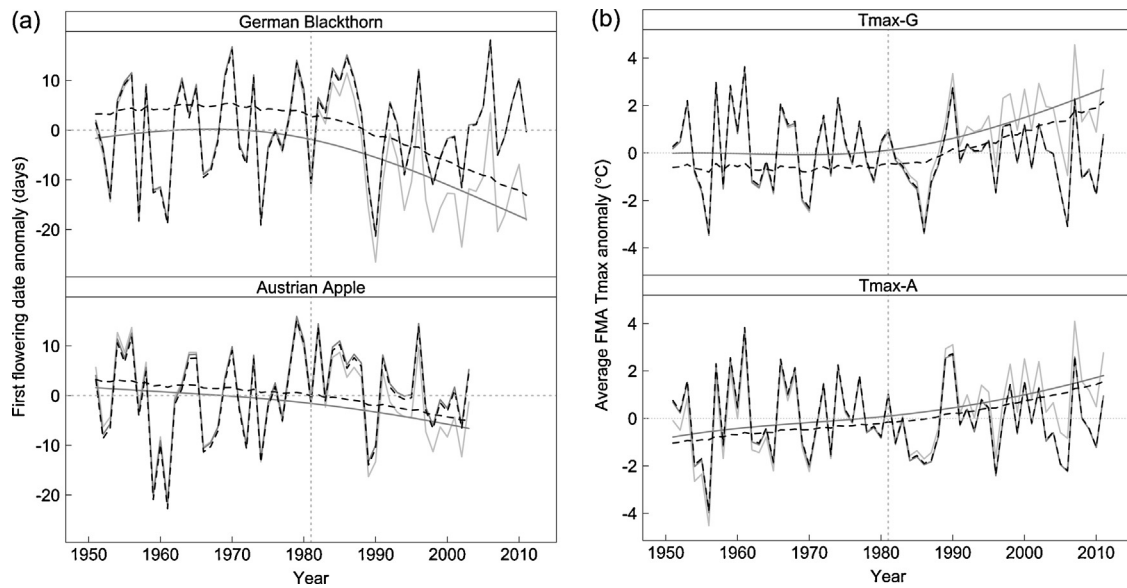


Fig. 2. (a) FFD and (b) average FMA T_{\max} anomalies (gray lines, base period 1961–1990). EEMD extracted OCs and trends are shown with dark gray lines, and PCA rotated OCs and trends are presented using black dashed lines. The vertical dotted lines indicate the year 1981.

and Matalas, 1964). The tests of significance for the Pearson's correlation coefficients (r) were based on the estimated edf.

3. Results

The results from empirical partial autocorrelation function indicated that all of the trends were 1st-order autoregressive, whereas none of the EEMD-extracted OCs was autocorrelated. All of the OCs and the corresponding trends were statistically uncorrelated over the examined time spans as well as over the split periods (see Appendix B).

3.1. Natural variability of temperature and FFD

The extracted OCs retained the year-to-year variability well (Table 2 and Fig. 2). Over the entire data span, regional average FMA T_{\max} OCs explained more than 75% of the variability in the corresponding FFD OCs (Fig. 3). For both species, the temperature sensitivities in P1 and P2 were not significantly different (all $P > 0.1$). Based on the OCs, the temperature sensitivity for the Austrian apple FFD was 4.63 ± 0.50 days (mean \pm se) per 1°C increase in $T_{\max-A}$ between 1981 and 2003. For the German blackthorn FFD, the sensitivity was 6.35 ± 0.80 days per 1°C increase in $T_{\max-G}$ over the same period (5.45 ± 0.36 days in P2).

Table 2

The detrended Pearson's correlation coefficients between the anomaly series and the corresponding EEMD-extracted OC.

Period	Apple FFD	$T_{\max-A}$
1951–2011 ^a	0.998 ^b	0.996
Before 1981	1.000	1.000
After 1981	1.000	0.999
	Blackthorn FFD	$T_{\max-G}$
1951–2011	0.970	0.969
Before 1981	0.998	1.000
After 1981	0.999	0.997

^a From 1951 to 2003 for the Austrian apple FFD series.

^b All $P < 0.001$. Except for the Apple FFD, the degrees of freedom for the tests of significance for the three periods are 59, 28, and 29, respectively. For the Apple FFD, the degrees of freedom for the three periods are 51, 28, and 21, respectively.

Three of the OCs were strongly correlated with the average January to March NAO_{GS} values, whereas the Austrian apple FFD OC was strongly correlated with the average January to April NAO_{GS} values (Fig. 4). Positive average winter/spring NAO_{GS} values led to higher regional average FMA T_{\max} and thus advanced the FFDs of both species. For all of the OCs, although their responses to the NAO in the split periods were not significantly different (all $P > 0.1$), the correlations with the average winter/spring NAO_{GS} index values were higher in P2 than in P1.

Three features emerged from analyzing the variances of all of the anomaly series and OCs. First, although the $T_{\max-A}$ and $T_{\max-G}$ had about the same amount of variability, the German blackthorn FFD was more variable than the Austrian apple FFD (Table 3). Second, the variances of the OCs were all smaller than that of the corresponding anomaly series in P2. Third, three of the anomaly series and all of the OCs were less variable in P2 than in P1.

3.2. Temperature and FFD trends

The EEMD-extracted trends in both Austrian series were more gradual and nearly linear over the study period. In contrast, the trends in the German series were close to the respective base period averages prior to 1981 and curved sharply afterwards (Fig. 2). The $T_{\max-G}$ trend was similar to the previous finding of a trend in the average FMA T_{mean} in a German region (Dose and Menzel, 2006). The extracted FFD trends were close to reverse images of the

Table 3

Variances of the anomaly series and EEMD-extracted OC.

Period	Apple FFD		$T_{\max-A}$	
	Anomaly	OC	Anomaly	OC
1951–2011 ^a	78.37 ^b	76.18	2.92	2.51
Before 1981	92.25	94.30	3.14	3.06
After 1981	61.81	52.50	2.39	2.04
	Blackthorn FFD		$T_{\max-G}$	
1951–2011	118.93	90.62	2.95	2.42
Before 1981	104.28	104.66	2.98	2.98
After 1981	105.40	80.07	2.59	1.90

^a From 1951 to 2003 for the Austrian apple FFD series.

^b The units for the FFD and T_{\max} series are days² and $^\circ\text{C}^2$, respectively.

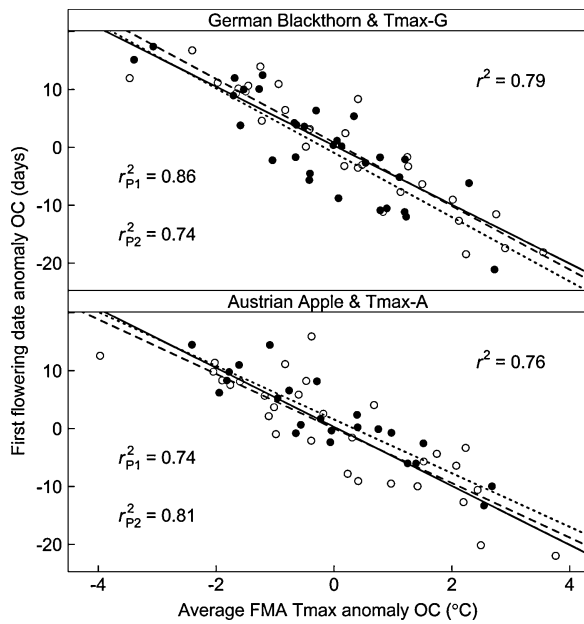


Fig. 3. Relationships between the OCs of FFD and the corresponding average FMA T_{max} anomalies. r^2 , r_{P1}^2 , and r_{P2}^2 are the coefficients of determination from the simple linear regressions for the entire data period (solid lines), before 1981 (opened circles and dashed lines), and after 1981 (solid circles and dotted lines), respectively.

corresponding average FMA T_{max} trends (Austrian apple and T_{max-A} $r = -0.996$, $P < 0.001$, $edf = 3.39$; German blackthorn and T_{max-G} $r = -0.995$, $P < 0.001$, $edf = 3.32$). The correlation strengths increased in P2 (Austrian apple and T_{max-A} $r = -1.000$, $P < 0.001$, $edf = 2.77$; German blackthorn and T_{max-G} $r = -0.997$, $P < 0.001$, $edf = 3.00$).

Based on the average first differences of the extracted trends, the Austrian apple and German blackthorn FFDs have advanced at rates of 0.225 ± 0.008 and 0.481 ± 0.014 day yr^{-1} in P2, respectively. For T_{max-A} and T_{max-G} , the warming rates were 0.056 ± 0.003 and 0.085 ± 0.005 $^{\circ}C yr^{-1}$ since 1981, respectively. The temperature sensitivity for the Austrian apple FFD was of 4.61 ± 0.06 days per $1^{\circ}C$ increase in T_{max-A} between 1981 and 2003, whereas the

Table 4

Proportion of variance explained by the principal components of the two EEMD-extracted components of each anomaly series.

Period	Apple FFD		T_{max-A}	
	PCA1 ^a	PCA2	PCA1	PCA2
1951–2011 ^a	0.93	0.07	0.84	0.16
Before 1981	0.99	0.01	0.98	0.02
After 1981	0.96	0.04	0.88	0.12
Period	Blackthorn FFD		T_{max-G}	
	PCA1 ^a	PCA2	PCA1	PCA2
1951–2011	0.77	0.23	0.77	0.23
Before 1981	1.00	0.00	1.00	0.00
After 1981	0.79	0.21	0.74	0.26

^a PCA1 is strongly correlated with the corresponding EEMD-extracted OC, whereas PCA2 is strongly correlated with the corresponding extracted trend (Fig. 2 and Appendix C).

^b From 1951 to 2003 for the Austrian apple FFD series.

sensitivity for the German blackthorn FFD was 6.22 ± 0.16 days per $1^{\circ}C$ increase in T_{max-G} over the same period (5.67 ± 0.08 days in P2).

3.3. Warming contribution toward FFD variability

The PCA results matched closely to the un-rotated components over both the entire data span and the split periods (Fig. 2 and Appendix C). The correlations between the anomaly series and the sum of the corresponding PCA components over the entire data span were all close to 1. Consequently, we can regard the proportions of variance explained by the rotated components as that of the un-rotated ones. Prior to 1981, almost all of the observed variability in each anomaly series was due to natural variability. However, the variability explained by the trends increased in P2, especially for the German series (Table 4). Because of the strong correlations between the FFD and average FMA T_{max} trends in P2, we can consider the proportions of variability explained by the FFD trends in P2 to have been contributed by recent warming. Thus, although the Austrian apple FFD variability in P2 was still primarily due to natural variability (96%), the rising T_{max-G} has contributed 21% of the blackthorn total FFD variability since 1981.

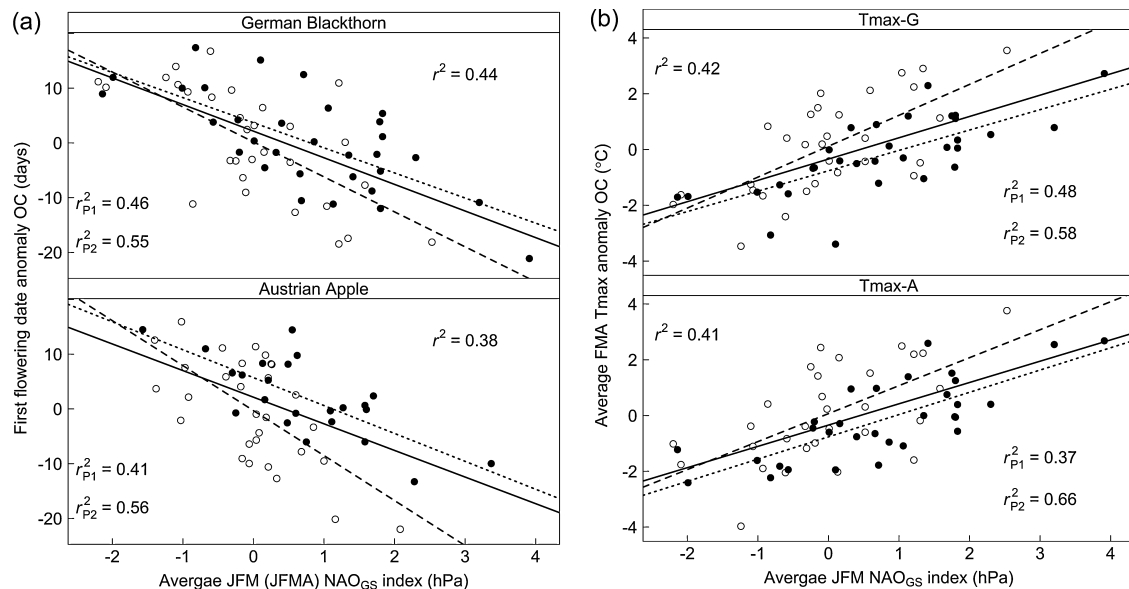


Fig. 4. Relationships between the average January to March (JFM) or January to April (JFMA, for the Austrian apple) NAO_{GS} index values and the OCs of (a) the FFD anomalies and (b) the average FMA T_{max} anomalies. Refer to Fig. 2 for legend.

4. Discussion

4.1. Rising temperature advances FFD

The extracted trends demonstrated unequivocally that recent winter/spring warming has indeed been responsible for advancing the FFDs of the two species. Moreover, none of the EEMD-extracted trends was linear (Fig. 2), which agrees with the findings based on Bayesian approach (e.g., Dose and Menzel, 2006; Pope et al., 2013). The results caution against using linear regressions to estimate warming and phenophase shifting rates. The trend-based approach used in this study provides an alternative for the purposes. Because the FFD temperature sensitivities estimated based on the OCs and trends were about equal for both species, the trend-based FFD advance rates should be reliable. The responses of both FFDs to the corresponding average FMA T_{\max} , however, were linear (Fig. 3).

4.2. Warming reduces both FFD and temperature natural variability

The FFD and average FMA T_{\max} OCs were less variable in P2, particularly for the German series (Table 3). A reduction in variance can be due to a lower oscillation frequency, amplitude, or both. Because of the limited series lengths, it is difficult to determine what the likely cause was. However, given no detectable changes in the NAO variability (Osborn, 2011) and the stronger correlations between the average winter/spring NAO_{GS} index and the OCs in P2 (Fig. 4), lower amplitudes were more likely to be the cause. While contributing toward the overall average FMA T_{\max} (and thus FFD) variability (Tables 3 and 4), the extra heat from recent warming also acted as a buffer modulating T_{\max} -A and T_{\max} -G natural fluctuation amplitudes. The FFD natural variations of both species were therefore reduced in response (Table 3 and Fig. 2). By concurrently shifting the timings and reducing the natural variability of a species' phenophase developments, recent warming may actually increase community-level phenophase variability, due to differential species responses (Cook et al., 2012; Diez et al., 2012). Future efforts in modeling phenophase responses to warming should consider incorporating the possible changes in temperature and phenophase temporal variability.

4.3. Differential warming rates and FFD responses

The contribution of the FFD trend for each species to the phenophase variability since 1981 was less than that of the corresponding average FMA T_{\max} trend to the temperature variability (Table 4). The results suggest that other factors have moderated the influence of the rising winter/spring temperature on the FFDs (Körner and Basler, 2010; Chuine et al., 2010; Cook et al., 2012). The difference in the proportions of the FFD variability explained by the warming trends in P2 is also considerable. Besides differential species responses to warming, the differential warming rates between the Austrian and the German sites (average 0.049 ± 0.002 vs. 0.075 ± 0.005 °Cyr⁻¹ over 1981–2003) may have also contributed to the difference. In addition to altitude, factors such as location, topography, and the degree of urbanization all can have a significant role in determining regional warming rates (Jochner et al., 2012; Cornelius et al., 2013).

4.4. Practical considerations using EEMD

Two issues need to be considered using EEMD, the number of Monte Carlo runs, and the standard deviation of the introduced Gaussian white noise. Although Wu and Huang (2009) states only a few hundred runs are necessary to achieve proper decompositions, this study found that a large number of runs was required

to cancel out the introduced noise. It is recommended that users of EEMD start with a few hundred runs and examine the absolute maximum, minimum, and mean deviations between the original data and the sum of EEMD result. If the deviations are unacceptable, then increase the number of runs. Because of its Monte Carlo nature, one can execute EEMD in parallel.

Without losing useful information, Wu and Huang (2009) recommends that the standard deviation of the Gaussian white noise to be 0.1 to 0.3 of that of the data. The standard deviations reported in this study were the ones that provided the best OC-trend separations. Again, users of EEMD should first start with the recommended values, then examine the results to see whether a proper OC-trend separation is achieved, which can be accomplished by using simple correlations.

5. Conclusions

The Earth's climate has clearly been warming during recent years, and plant phenophases have shifted in response in many temperate ecosystems. As this study has shown, warming can affect both the timing and the natural variability of a phenophase development. It will be of great interest and importance to examine whether the conclusion holds for other phenophases and species in various regions as well. The EEMD approach will be a valuable tool for answering the question.

Acknowledgments

The Austrian and German FFD data were provided by the members of the PEP725 project. The author acknowledges the EU-FP6 project ENSEMBLES (Contract number 505539) and the data providers in the ECA & D project (<http://eca.knmi.nl>) for the use of the E-OBS dataset. Comments from WEW, BMB, and ERC are also acknowledged. This study was supported by Taiwan National Science Council (NSC97-2627-M-002-021, NSC97-2621-B-002-002-MY3, and NSC101-2313-B-002-015-MY3) and by National Taiwan University.

References

- Amano, T., Smithers, R.J., Sparks, T.H., Sutherland, W.J., 2010. A 250-year index of first flowering dates and its response to temperature changes. *Proc. R. Soc. London, Ser. B* 277, 2451–2457.
- Badeck, F.-W., Bondeau, A., Böttcher, K., Doktor, D., Lucht, W., Schaber, J., Sitth, S., 2004. Responses of spring phenology to climate change. *New Phytol.* 162, 295–309.
- Chmielewski, F.-M., Rötzer, T., 2001. Response of tree phenology to climate change across Europe. *Agric. For. Meteorol.* 108, 101–112.
- Chuine, I., Morin, X., Bugmann, H., 2010. Warming, photoperiods, and tree phenology. *Science* 329, 277–278.
- Cleland, E.E., Chuine, I., Menzel, A., Mooney, H.A., Schwartz, M.D., 2007. Shifting plant phenology in response to global change. *Trends Ecol. Evol.* 22, 357–365.
- Cook, B.L., Wolkovich, E.M., Parmesan, C., 2012. Divergent responses to spring and winter warming drive community level flowering trends. *Proc. Nat. Acad. Sci. U.S.A.* 109, 9000–9005.
- Cornelius, C., Estrella, N., Franz, H., Menzel, A., 2013. Linking altitudinal gradients and temperature responses of plant phenology in the Bavarian Alps. *Plant Biol.* 15 (Suppl. 1), 57–69.
- Dawdy, D.R., Matalas, N.C., 1964. Statistical and probability analysis of hydrologic data, Part III: Analysis of variance, covariance and time series. In: Chow, V.T. (Ed.), *Handbook of Applied Hydrology, A Compendium of Water-Resources Technology*. McGraw-Hill, New York, NY, pp. 8.68–8.90.
- Diez, J.M., Ibáñez, I., Miller-Rushing, A.J., et al., 2012. Forecasting phenology: from species variability to community patterns. *Ecol. Lett.* 15, 545–553.
- Donnelly, A., Caffarra, A., O'Neill, B.F., 2011. A review of climate-driven mismatches between interdependent phenophases in terrestrial and aquatic ecosystems. *Int. J. Biometeorol.* 55, 805–817.
- Dose, V., Menzel, A., 2006. Bayesian correlation between temperature and blossom onset data. *Global Change Biol.* 12, 1451–1459.
- Golyandina, N., Zhigljavsky, A., 2013. *Singular Spectrum Analysis for Time Series*. Springer, New York, NY.
- Haylock, M.R., Hofstra, N., Klein Tank, A.M.G., Klok, E.J., Jones, P.D., New, M., 2008. A European daily high resolution gridded data set of surface

- temperature and precipitation for 1950–2006. *J. Geophys. Res.* 113, D20119, <http://dx.doi.org/10.1029/2008JD010201>.
- Huang, N.E., Wu, Z., 2008. A review on Hilbert–Huang transform: method and its applications to geophysical studies. *Rev. Geophys.* 46, RG2006, <http://dx.doi.org/10.1029/2007RG000228>.
- Huang, N.E., Shen, Z., Long, S.R., et al., 1998. The empirical mode decomposition and the Hilbert spectrum for nonlinear and non-stationary time series analysis. *Proc. R. Soc. London, Ser. A* 454, 903–995.
- Hudson, I.L., Keatley, M.R., 2010. Singular spectrum analysis: climatic niche identification. In: Hudson, I.L., Keatley, M.R. (Eds.), *Phenological Research: Methods for Environmental and Climate Change Analysis*. Springer, Dordrecht, pp. 393–424.
- Jochner, S.C., Sparks, T.H., Estrella, N., Menzel, A., 2012. The influence of altitude and urbanisation on trends and mean dates in phenology (1980–2009). *Int. J. Biometeorol.* 56, 387–394.
- Jones, P., Jonsson, T., Wheeler, D., 1997. Extension to the North Atlantic Oscillation using early instrumental pressure observations from Gibraltar and South-West Iceland. *Int. J. Climatol.* 17, 1433–1450.
- Körner, C., Basler, D., 2010. Phenology under global warming. *Science* 327, 1461–1462.
- Memmott, J., Craze, P.G., Waser, N.M., Price, M.V., 2007. Global warming and the disruption of plant–pollinator interactions. *Ecol. Lett.* 10, 710–717.
- Menzel, A., 2003. Plant phenological anomalies in Germany and their relation to air temperature and NAO. *Clim. Change* 57, 243–263.
- Menzel, A., 2006. European phenological response to climate change matches the warming pattern. *Global Change Biol.* 12, 1969–1976.
- Osborn, T.J., 2011. Variability and changes in the North Atlantic Oscillation Index. In: Vicente-Serrano, S.M., Trigo, M. (Eds.), *Hydrological, Socioeconomic and Ecological Impacts of the North Atlantic Oscillation in the Mediterranean Region*. Springer, New York, NY, pp. 9–22.
- Paige, R.L., Trindade, A.A., 2010. The Hodrick–Prescott filter: a special case of penalized spline smoothing. *Electron. J. Stat.* 4, 856–874.
- Parmesan, C., 2007. Influences of species, latitudes and methodologies on estimates of phenological response to global warming. *Global Change Biol.* 13, 1860–1872.
- Parmesan, C., Yohe, G., 2003. A globally coherent fingerprint of climate change impacts across natural systems. *Nature* 421, 37–42.
- Parmesan, C., Duarte, C., Poloczanska, E., Richardson, A.J., Singer, M.C., 2011. Overstretching attribution. *Nat. Clim. Change* 1, 2–4.
- Pan European, 2012. PEP725 Pan European Phenology Project. Pan European, <http://www.zamg.ac.at/pep725/> (last accessed 3 July 2012).
- Polgar, C.A., Primack, R.B., 2011. Leaf-out phenology of temperate woody plants: from trees to ecosystems. *New Phytol.* 191, 926–941.
- Pope, K.S., Dose, V., Da Silva, D., Brown, P.H., Leslie, C.A., DeJong, T.M., 2013. Detecting nonlinear response of spring phenology to climate change by Bayesian analysis. *Global Change Biol.* 19, 1518–1525.
- Root, T.L., Price, J.T., Hall, K.R., Schneider, S.H., Rosenzweig, C., Pounds, J.A., 2003. Fingerprints of global warming on wild animals and plants. *Nature* 421, 57–60.
- Rosenzweig, C., Karoly, D., Vicarelli, M., et al., 2008. Attributing physical and biological impacts to anthropogenic climate change. *Nature* 453, 353–357.
- Schleip, C., Rutishauser, T., Luterbacher, J., Menzel, A., 2008. Time series modeling and central European temperature impact assessment of phenological records over the last 250 years. *J. Geophys. Res.* 113, G04026, <http://dx.doi.org/10.1029/2007JG000646>.
- Schwartz, M.D., Ahas, R., Aasa, A., 2006. Onset of spring starting earlier across the Northern Hemisphere. *Global Change Biol.* 12, 343–351.
- Walther, G.-R., 2010. Community and ecosystem responses to recent climate change. *Philos. Trans. R. Soc. London, Ser. B* 365, 2019–2024.
- Wu, Z., Huang, N.E., 2009. Ensemble empirical mode decomposition: a noise assisted data analysis method. *Adv. Adapt. Data Anal.* 1, 1–41.
- Wu, Z., Huang, N.E., Long, S.R., Peng, C.K., 2007. On the trend, detrending, and variability of nonlinear and nonstationary time series. *Proc. Nat. Acad. Sci. U.S.A.* 104, 14889–14894.